Multi-omics comprehensive analysis reveals the predictive value of N6-methyladenosine-related genes in prognosis and immune escape of bladder cancer

Yang Liu[a,b,1], Zhongqi Pang[b,1], Jianshe Wang[b,1], Jinfeng Wang[b], Bo Ji[b], Yidan Xu[b], Jiaxin He[b], Lu Zhang[b], Yansong Han[b], Linkun Shen[b], Wanhai Xu[c,*] and Minghua Ren[b,*]

[a]*Department of Urology, The Eighth Affiliated Hospital of Sun Yat-Sen University, Shenzhen, Guangdong, China*
[b]*Department of Urology, The First Affiliated Hospital of Harbin Medical University, Harbin, Heilongjiang, China*
[c]*Department of Urology, The Fourth Affiliated Hospital of Harbin Medical University, Harbin, Heilongjiang, China*

Abstract.

BACKGROUND: N6-methyladenosine (m6A) is the most frequent RNA modification in mammals, and its role in bladder cancer (BC) remains rarely revealed.

OBJECTIVE: To predict the value of m6A-related genes in prognosis and immunity in BC.

METHODS: We performed multiple omics analysis of 618 TCGA and GEO patients and used principal component analysis (PCA) to calculate the m6A score for BC patients.

RESULTS: We described the multiple omics status of 23 m6A methylation-related genes (MRGs), and four m6A clusters were identified, which showed significant differences in immune infiltration and biological pathways. Next, we intersected the differential genes among m6A clusters, and 11 survival-related genes were identified, which were used to calculate the m6A score for the patients. We found that the high-score (HS) group showed lower tumor mutation burden (TMB) and TP53 mutations and better prognosis than the low-score (LS) group. Lower immune infiltration, higher expression of PD-L1, PD-1, and CTLA4, and higher immune dysfunction and immune exclusion scores were identified in the LS group, suggesting a higher possibility of immune escape. Finally, the experimental verification shows that the m6A related genes, such as IGFBP1, plays an important role in the growth and metastasis of bladder cancer.

CONCLUSIONS: These findings revealed the important roles of m6A MRGs in predicting prognosis, TMB status, TP53 mutation, immune functions and immunotherapeutic response in BC.

Keywords: N6-methyladenosine, bladder cancer, prognosis, immunotherapy, m6A score

Abbreviations

BC	bladder cancer
ICIs	immune checkpoint inhibitors
m6A	N6-methyladenosine
MRGs	methylation-related genes
TMB	tumor mutation burden
TCGA	The Cancer Genome Atlas
GEO	Gene Expression Omnibus
PCA	principal components analysis

---

[1]First authors.

*Corresponding authors: Wanhai Xu, Department of Urology, The Fourth Affiliated Hospital of Harbin Medical University, Harbin, Heilongjiang 150001, China. E-mail: xuwanhai@hrbmu.edu.cn. Minghua Ren, Department of Urology, The First Affiliated Hospital of Harbin Medical University, Harbin, Heilongjiang 150007, China. Tel.: +86 13946119939; E-mail: 002051@hrbmu.edu.cn.

CNV   copy number variation
DEGs   differentially expressed genes
OSRGs   OS-related genes
IGF   insulin-like growth factor
HS group   high-score group
LS group   low-score group
PPI   protein-protein interaction
GO   Gene Ontology
KEGG   Kyoto Encyclopedia of Genes and
           Genomes
GSEA   Gene set enrichment analysis
DSS   Disease-specific survival
OS   Overall survival

1. Introduction

Bladder cancer (BC) is among the top 10 malignancies worldwide, with the highest incidence and mortality in the urinary system, which places a heavy burden on society as a whole [1,2]. At present, the initiation mechanism of BC is still unclear. somehow, several risk factors, such as age, gender, cigarettes, chemical contact, heredity and other elements, have been identified [3]. So far, the common therapies for BC, including surgery, chemotherapy, and immune therapy, have achieved great improvement in BC prognosis, but many BC patients still suffer from high recurrence possibilities, even with noneffective methods for advanced or metastatic BC [4]. Therefore, investigating novel methods that could help with the early diagnosis of BC or predict prognosis is urgently needed.

N6-methyladenosine (m6A) is the most frequent RNA modification in mammalian cells [5]. The basic m6A process includes 3 types of genes and their downstream proteins: writers (such as METTL3, METTL14, METTL16, WTAP, VIRMA, ZC3H13, RBM15 and RBM15B), readers (such as YTHDC1, YTHDC2, YTHDF1, YTHDF2, YTHDF3, HNRNPC, FMR1, LRPPRC, HNRNPA2B1, IGFBP1, IGFBP2, IGFBP3 and RBMX), and erasers (such as FTO and ALKBH5), which add, identify and delete m6A-modified sites [6]. These m6A regulation genes are reported to play important roles in tumorigenesis and tumor progression [7,8, 9]. For example, it has been reported that knockdown of METTL3 (one of the writers) inhibits BC cells *in vitro* and tumorigenesis *in vivo*, while overexpression of METTL3 improves BC invasion [10]. Meanwhile, the high expression of YTHDF2 (one of the readers) has a close relationship with poor survival, and cell proliferation and migration were significantly inhibited

after knocking down YTHDF2 in prostate cancer [11]. Additionally, FTO (one of the erasers) is known as an oncogene that is closely associated with BC progression [12]. Obviously, these findings suggest the important roles of m6A regulatory genes in tumors.

Immunotherapy has become an important treatment strategy in BC, especially advanced BC and metastatic BC, which has ameliorated the prognosis. Currently, immune checkpoint inhibitors (ICIs) are the first-line treatment for BC, and PD-1, PD-L1 and CTLA4 expression levels are considered to be associated with the immunotherapy response [13]. Although ICIs have made great improvements in BC prognosis, only a few patients gain clear benefit from ICI treatment, and some patients suffer side effects and medicine toxicity [14]. Therefore, it is imperative to explore novel effective therapeutic methods and molecular targets to improve the immunotherapy effect of patients. Interestingly, it has been reported that BC patients who have high CD8+ T-cell infiltration levels with a high tumor mutation burden (TMB) could gain more benefit from ICI treatment [15]. At the same time, TP53 mutation is believed to be associated with disease progression and poor prognosis of BC [16]. Undoubtedly, it can be seen that poor prognosis of tumors is the result of the comprehensive effect of tumor immunity, gene mutation, gene expression and other factors, which suggests that early identification and intervention of these factors may be a feasible method to improve the prognosis of cancer, including BC.

Liu et al. showed the importance of the multiomic characteristics of m6A related genes in exploring the biological function of bladder cancer. Due to the complex functions of m6A related genes, more evidence needs to be further explored [17]. In this work, we aimed to reveal the important roles of m6A methylation-related genes (MRGs) in predicting prognosis, TMB status, TP53 mutation, immune functions and immunotherapeutic response in BC and to offer novel molecular targets for the precision treatment of BC.

2. Material and methods

2.1. Data sources

In this work, transcriptome data, single nucleotide polymorphism (SNP) data, copy number variation (CNV) data and related clinical information were downloaded from the TCGA database (https://tcga-data. nci.nih.gov/tcga/) for 430 cases (411 BC cases and

19 normal cases). Firstly, raw data of each case was extracted and generated a matrix by using Perl software. Then, case IDs were conformed into a consistent layout, as well as annotated gene names accurately in the matrix. Next, a standardized transcriptomic matrix was generated by applying formula log2 (x + 1) for further investigation. The clinical information (Supplementary Table 1) was first examined to obliterate any duplicates or missing data, then matched with transcriptomic data of each case for further analysis. As for the SNPs data, it could be directly used after matching with the patient ID of transcriptome data. Meanwhile, transcriptome data and clinical information (Supplementary Table 2) of 188 BC cases were obtained from the GSE13507 dataset (https://www.ncbi.nlm.nih.gov/geo/query/acc.cgi?acc=GSE13507). The transcriptome data was annotated by using platform file GPL6102, deleting missing data and standardized these data by applying formula log2 (x + 1) for further investigation. The clinical information was examined to delete duplicating and missing data for further analysis.

2.2. Identification of differentially expressed genes

Before analysis, we standardized all transcriptomics data by applying log2 (x + 1). Then, we applied the edge R package with FDR < 0.05 and |log2FC| ⩾ 1 to identify differentially expressed genes (DEGs) of transcriptomics in both the TCGA and GEO cohorts.

2.3. Protein-protein interaction network

We generated a protein-protein interaction network (PPI) for MRGs by using STRING (https://string-db.org/) and Cytoscape software.

2.4. Enrichment analysis

We applied Gene Set Variation Analysis (GSVA), Gene Ontology (GO) and Kyoto Encyclopedia of Genes and Genomes (KEGG) for functional or pathway enrichment analysis. Briefly, expression profiles of DEGs or MRGs were put into R software to perform the enrichment analysis, calculating enrichment scores, estimating significance levels and performing multiple hypothesis, which finally indicated the potential gene functions and pathways.

2.5. M6A scores were evaluated for patients

Principal components analysis (PCA) is an effective

technique for reducing data dimensionality. Calculation steps (assuming that the sample data is n-dimensional, with a total of m): 1. Organize these sample data into a matrix Xnm by column; 2. Row-wise averaging X, which means first calculating the average value of each row, and then subtracting this average value from each element in that row; 3. Calculate the covariance matrix; 4. Find the eigenvalues of the covariance matrix, which are the corresponding eigenvectors; 5. Arrange the feature vectors into a matrix by row from top to bottom according to the corresponding feature values, and take the first k rows to form a matrix P; 6. Then Y = PX is the data set after dimensionality reduction to k. These steps are ultimately accomplished with the help of R package. In this work, we first used PCA to analyze the expression of 11 survival-related genes (CLIC4, KPNA2, PAQR4, MTHFD2, CDC25B, WDR62, TPX2, CRTAC1, KLHL3, SMAD6, ZNF552) and obtained the corresponding PCA score. Next, we calculated the m6A score of each patient according to the PCA score: m6A score = pca (1) + pca (2) + ... + pca (n). Finally, patients were divided into a high score (HS) group and a low score (LS) group according to the m6A score in both the TCGA and GEO cohorts for subsequent analysis.

2.6. Cell culture

In this study, human bladder cancer cell lines UMUC3 and RT112 were cultured in RPMI-1640 (Gibco, USA) supplemented with 10% fetal bovine serum and 1% penicillin/streptomycin, as well as cultured at 37°C and in 5% CO_2.

2.7. Transfection assay

We obtained the overexpression plasmid of IGFBP1 and paired empty plasmid from GeneCopoeia (Guangzhou, China). Firstly, we planted BC cells into 6-well plates and waited for cell density reached at 80%–90%. Then, we changed the culture medium into 1.5 ml Opti-MEM (Gibco) for each well at two hours before transfection. Meanwhile, we set two groups for transfection: negative control group (NC) and knockdown group (SH). For each well in SH group, 10 ul IGFBP1 knockdown plasmid was added into 240 ul Opti-MEM, as well as 5 ul lipo2000 (Thermo, USA) was supplanted into 245 ul Opti-MEM and set still at room temperature for 5 minutes. Next, we mixture plasmid solution with lipo2000 solution and set still at room temperature for 10 minutes, following adding

total 500 ul transfection solution into 1.5 ml Opti-MEM culture medium to form 2 ml volume transfection system in each well. The NC group followed the same protocol but changed the knockdown plasmid into empty plasmid. After 8 hours transfection, we changed the transfection culture medium into 2 ml RPMI-1640 supplemented with 10% serum. The transfected efficacy was confirmed by examining the fluorescence percentage. We chose the wells that had a minimum of 80% fluorescence percentage for further investigation.

2.8. RT-PCR

The reactions were performed on the QuantStudio 5 Real-Time PCR instrument (Thermo Fisher, USA) using 2x SYBR Green Pro Taq HS Premix II (AgBio, China). Normalization of mRNA levels was against GAPDH levels. For calculating the relative gene expression, the 2-$\Delta\Delta$CT approach was employed. (First, for all test samples and calibration samples, the CT value of the internal reference gene is normalized to the CT value of the target gene: ΔCT test = CT target, test – CT ref, test; ΔCT calibrator = CT target, calibrator CT ref, calibrator. Second, normalize the ΔCT value of the test sample with the ΔCT value of the calibration sample: $\Delta\Delta$CT = ΔCT test – ΔCT calibrator. Finally, calculate the expression level ratio: $2-\Delta\Delta$CT = the ratio of the amount of expression.)

2.9. CCK8 assay

This assay was followed by the protocol of Beyotime CCK8 kit. Briefly, we adjusted the cell density of transfected and control cells to 5000/100 ul. Then, we added 100 ul cell suspension into each well of 96-well plate, supplemented with 10 ul CCK8 solution, and cultured at 37°C for one hour. Afterward, we examined the optical density at 450 nm wavelength to examine the cell proliferation. This assay was repeated at least three times.

2.10. Wound healing assay

We seeded the transfected cells into six-well plates and waited for the cell density reaching more than 90%. Then we scratched several vertical lines by using a 200 ul pipette tip. After three times washing with PBS solution, we changed the culture medium to 2 ml serum-free culture medium. Photos of this assay at 0 hour, 24 hour were taken to examine the wound healing rates.

2.11. Transswell assay

The transfected cells were incubated in serum-free medium for 12 h and then adjusted to a density of $1*10^6$ cells/ml. Next, 200 mL of cell suspension was added to the transwell chambers (Corning, NO.3422), which were fit into the wells of 24-well plates. The wells of the plates also each contained 500 ml of RPMI-1640 medium supplemented with 10% FBS. After 24 hours of incubation, cells on the upper membrane were removed with cotton wool, whereas cells adhering to the lower surface were fixed in methanol for 30 min and then stained with 0.1% crystal violet for 10 minutes. After natural air drying, the migrating cells on the lower surface of the membrane were counted under an optical microscope at 200 folds magnification.

2.12. Statistical analysis

We employed one-way ANOVA and t tests for comparisons between groups, and the comparison of two or more constituent ratios was performed by the chi-square test. Correlation analysis, heatmap, waterfall curve and box plots were completed by R software (version 3.5.1). We processed all statistical analyses by applying SPSS 19.0 software (SPSS. Inc., Chicago, IL, USA) or R software. In this work, we set the significance level to $P <$ 0.05.

3. Results

3.1. Multi-omics biological characteristics of m6A MRGs and its relationship with survival in BC

First, we investigated the CNV status of 23 m6A MRGs in TCGA patients with BC. The results showed that 56.52% (13/23) of m6A-related genes gained more CNV frequencies than they lost, and VIRMA had the highest frequency. In contrast, 43.48% (10/23) of genes lost more CNV frequencies than they gained, and YTHDF2 had the top percentage (Supplementary Fig. 1A). Moreover, the localization of these genes in the chromosome was described as well (Supplementary Fig. 1B). Then, we found a good protein-protein interaction network, which revealed a potential regulatory relationship among these genes (Supplementary Fig. 1C). Next, we compared the expression statuses of these genes from 411 BC cases with 19 normal cases and found that HNRNPA2B1 and HNRNPC had the most significant differences (Supplementary Fig. 1D). After that, we found that these 23 genes were mutated in 24.51% of 411 TCGA BC patients, of which METTL3 was the most frequently mutated (Supple-
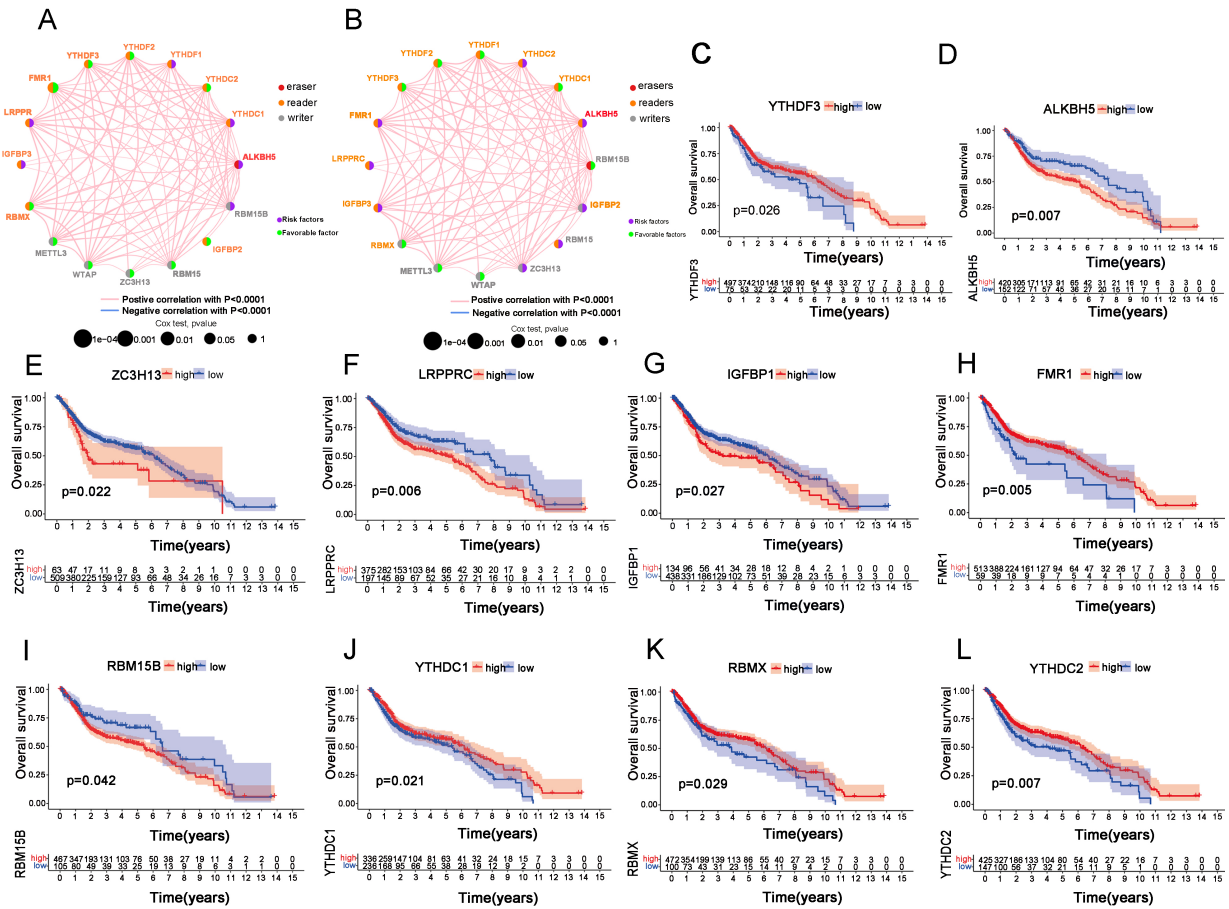
Fig. 1. m6A MRGs significantly affect the survival of bladder cancer patients. (A, B) Overall survival (OS) and disease-specific survival (DSS) prognostic networks were constructed according to 17 MRGs. (C–I) Kaplan-Meier analysis of OS for m6A MRG genes.

mentary Fig. 1E). Furthermore, we investigated the expression status of 22 other genes when the METTL3 gene was mutated or not. The results showed that 17 genes were differentially expressed in METTL3 mutant or wild-type cells, and the results of RBM15 and YHDF2 are shown as examples (Supplementary Fig. 1F and G), which indicated that METTL3 was one of the key m6A MRGs in BC.

We combined 411 BC cases in TCGA and 188 GEO BC cases and finally identified 17 MRGs with complete data for subsequent analysis. Next, we constructed overall survival (OS) and disease-specific survival (DSS) prognostic networks according to these 17 MRGs (Fig. 1A and B). More precisely, the networks exhibited the detailed function of these MRGs in m6A methylation (erasers, readers or writers), as well as the correlation between genes and the role of the gene as a protective or risk factor in OS and DSS. Then, we investigated every single gene by Kaplan-Meier analysis and finally found that ALKBH5, ZC3H13, LRP-

PRC, IGFBP1, and RBM15B were associated with poor OS and that FMR1, YTHDF3, YTHDC1, RBMX and YTHDC2 were associated with better OS (Fig. 1C–L). Additionally, we performed Kapan-Meier analysis for DSS and found that 9 of 17 MRGs were statistically significant (Supplementary Fig. 2A–I). All these findings highlight the important roles of m6A MRGs in the prognosis of BC.

3.2. m6A clusters were identified based on MRGs in BC patients

Based on the gene expression of these 17 m6A MRGs, a consensus clustering analysis was performed for 596 BC cases (408 from TCGA and 188 from GEO), and the results showed that our patients were well divided into 4 m6A clusters when $k = 4$ (Fig. 2A). After that, we found that these MRGs showed apparent differences among the four groups of patients (Fig. 2B).
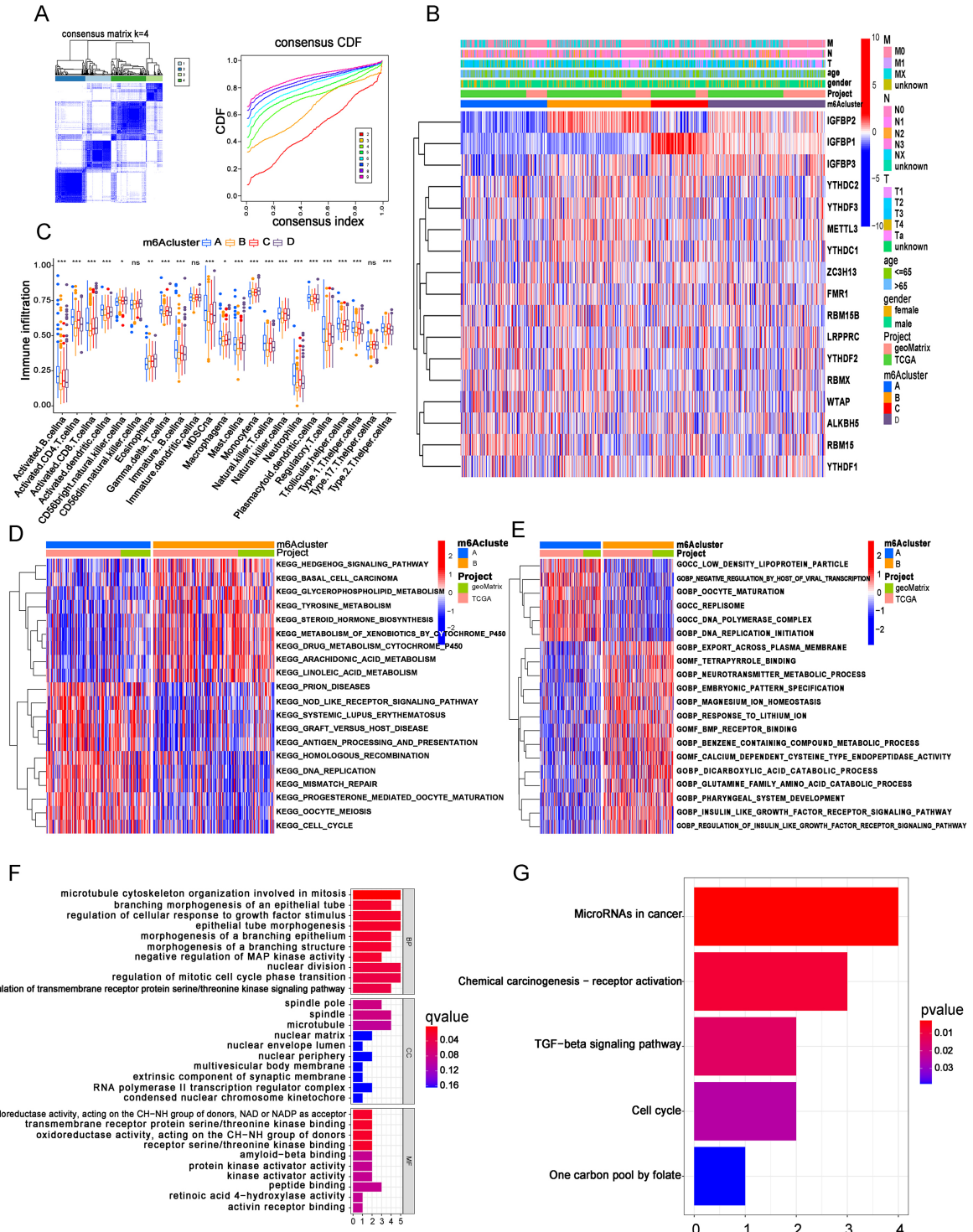
Fig. 2. m6A clusters were identified based on MRGs in BC patients. (A) BC samples ($n = 596$) were divided into four m6A clusters based on the consensus clustering matrix ($k = 4$) in both TCGA and GEO cohorts. (B) Heatmap of the expression status of 17 m6A MRGs in m6A clusters. (C) The differences in 23 immune cell infiltration levels in m6A clusters. (D, E) KEGG and GO functional analysis between m6A clusters A and B. (F, G) The results of GO and KEGG enrichment analysis for the intersection of differentially expressed genes between m6A clusters.

Then, a boxplot for immune infiltration status was generated based on the m6A clusters (Fig. 2C). According to the results, we noticed significant differences in immune cell infiltration among the 4 m6A clusters of patients. More specifically, m6A cluster A had a high level of immune cell infiltration (such as CD4+ T cells, CD8+ T cells, NK cells and B cells), suggesting good immune function. In contrast, m6A cluster D had a poor level of immune infiltration, suggesting poor immune function. After that, ssGSEA was performed to explore the underlying functions or pathways for these clusters. KEGG analysis showed that metabolism-related pathways, such as linoleic acid metabolism, were significantly downregulated in cluster A compared with cluster B, while tumor-related pathways, such as DNA replication pathways and cell cycle pathways, were apparently upregulated in cluster A (Fig. 2D). In addition, similar results were observed in KEGG analysis of comparisons between cluster A and other m6A clusters (Supplementary Fig. 3A and B). Accordingly, these enriched pathways could partly explain the reason for the worst prognosis and lowest m6A score of patients in cluster A based on the results from the subsequent analysis of our work. In addition, we conducted pairwise comparisons of different KEGG pathways between m6A clusters (Supplementary Fig. 3C–E).

Consistently, we also performed GO functional analysis between m6A clusters. From the results of the comparison between clusters A and B, we noticed that several GO biological processes (GOBP), such as DNA replication initiation, and GO cellular components (GOCC), such as replisome, were at higher levels in cluster A, while some GOBPs and GO molecular functions (GOMF) were downregulated in cluster A. Interestingly, we noticed that insulin-like growth factor (IGF)-related GOBP levels were lower in patients from cluster A, whose prognosis and m6A score were the worst, while IGF levels were commonly upregulated in advanced malignancies (Fig. 2E) [17,18]. Nevertheless, comparisons of GO function analysis between cluster A and other m6A clusters were also performed (Supplementary Fig. 4A and B). In addition, we also conducted pairwise comparisons of GO functions between other m6A clusters (Supplementary Fig. 4C–E). After that, we distinguished the differentially expressed genes by comparing every two m6A clusters (clusters A and B, A and C, A and D, B and C, B and D, and C and D) and further intersected these differentially expressed genes among these comparisons to process Unicox analysis, which finally identified 11 OS-related genes (OSRGs) (CRTAC1, SMAD6, CDC25B,

ZNF552, KLHL3, TPX2, WDR62, MTHFD2, PAQR4, KPNA2 and CLIC4). Additionally, we employed GO and KEGG enrichment analysis for these 11 OSRGs. We found that these genes were mainly enriched in microtubule cytoskeleton organization involved in mitosis, regulation of cellular response to growth factor stimulus and epithelial tube morphogenesis (Fig. 2F). At the same time, we noticed that OSRGs were mainly enriched in microRNAs in cancer, as well as TGF-β signaling pathways and cell cycle pathways (Fig. 2G), which revealed that these OSRGs were involved in tumorigenesis-related pathways and could apparently alter prognosis. Therefore, these findings reveal the important value of m6A MRGs in identifying immune cell infiltration and prognosis in BC patients and highlight OSRGs as tumor-related genes.

3.3. m6A score was established to predict the prognosis of BC patients

To further investigate the roles of these 11 OSRGs in our patients, a new consensus clustering analysis was performed. When $k = 2$, cases could be well separated so that these 596 BC cases were divided into 2 gene clusters (Fig. 3A). As shown in Fig. 3B, these 11 OSRGs were apparently different in gene expression between the 2 gene clusters, and the details are shown in Fig. 3C. To be more precise, we found that the expression levels of CRTAC1, SMAD6, ZNF552 and KLHL3 were higher in gene cluster B than in gene cluster A, while the others showed the opposite results. Then, we followed Kapan-Meier analysis for OS and DSS separately based on the gene clusters (Fig. 3D and E). The results showed that patients in gene cluster B had a better prognosis than patients in gene cluster A, which demonstrated the ability of these genes to predict the prognosis of BC patients. Furthermore, we calculated the m6A score of each case via principal component analysis (PCA) and divided them into a high-score (HS) group and a low-score (LS) group. Next, we ran Kapan-Meier analysis for OS and DSS based on m6A score groups separately (Fig. 3F and G) and found that patients in the HS group had better survival possibilities than those in the LS group. Surprisingly, we observed the same survival trends among groups with consistent clinical parameters (T grades, N grades, age and sex, etc.) (Supplementary Fig. 5A–H). In addition, we further investigated the clinical characteristics of these BCs between m6A score groups. As the results showed, patients in the HS group had less mortality than those in the LS group, and patients in the HS group showed
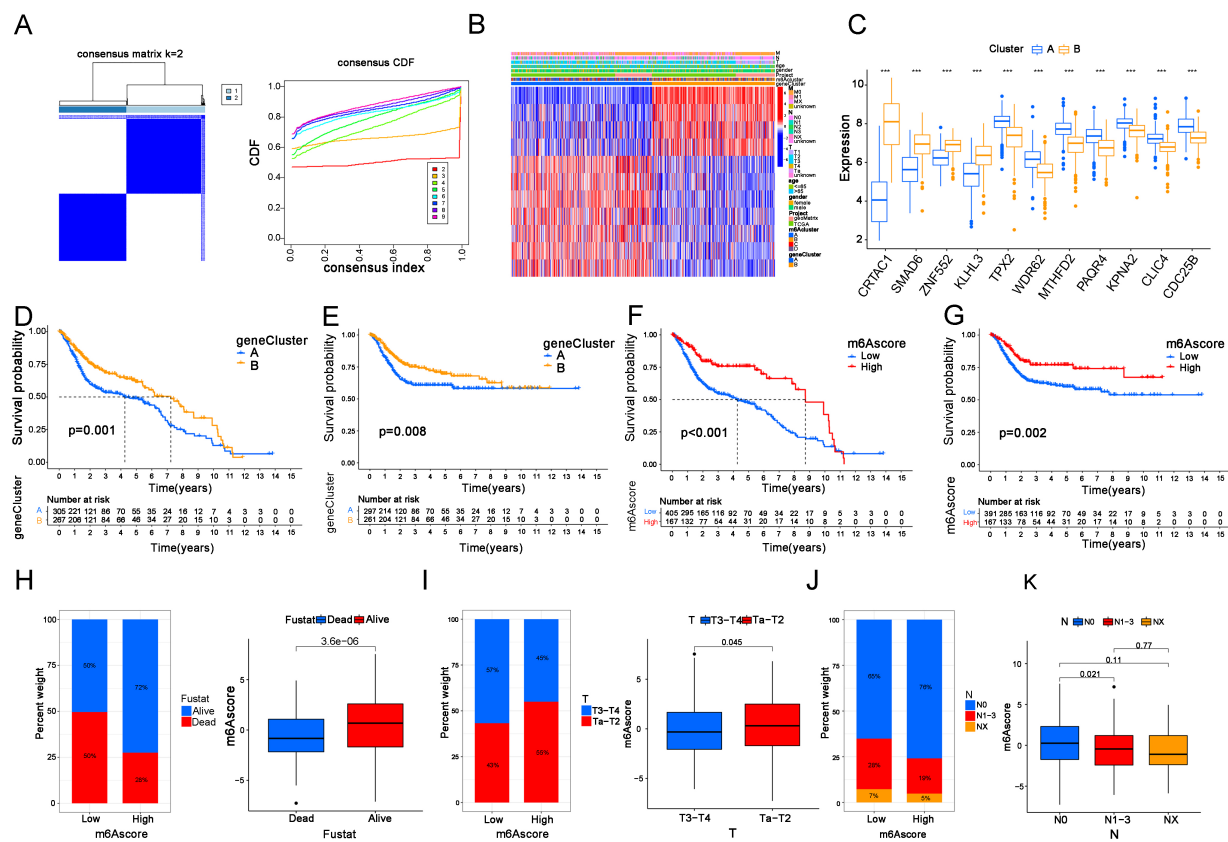
Fig. 3. The m6A score was established to predict the prognosis of BC patients. (A) BC samples ($n = 596$) were separated into two gene clusters based on the consensus clustering matrix ($k =2$) in both TCGA and GEO cohorts. (B) Heatmap of 11 survival-related gene expression statuses between gene clusters. (C) Boxplot of 11 survival-related gene expression levels between gene clusters. (D, E) Kaplan-Meier analysis for OS (D) and DSS (E) between gene clusters. (F, G) Kaplan-Meier analysis of OS (F) and DSS (G) between the HS group and LS group. (H–J) Living status (H), T grade (I) and N grade (J) in the m6A score groups.

lower T stage and N stage than those in the LS group (Fig. 3H–J). These findings demonstrated the ability of the m6A score to predict the prognosis of BC patients.

3.4. m6A score is closely related to TMB and gene mutations in BC patients

First, we examined the relationship between the m6A score and m6A clusters and gene clusters (Fig. 4A and B). From the results, we found that patients in m6A cluster B, m6A cluster D and gene cluster B had higher m6A scores, suggesting a better prognosis, which is basically consistent with our previous conclusion. Next, a more intuitive Sankey diagram showed the corresponding relationship among the m6A cluster, gene cluster, m6A score and fustat status among 596 BC cases (Fig. 4C). Next, we found that the m6A score was negatively correlated with the TMB level, and the HS group was associated with a lower TMB level than

the LS group (Fig. 4D and E). Then, we investigated the prognosis of BC with high and low TMB levels via Kaplan-Meier analysis for OS. Surprisingly, the results showed that patients with higher TMB levels gained better survival possibilities than those with lower TMB levels (Fig. 4F). Moreover, patients with high TBM and high m6A scores had the best prognosis, while patients with low TMB and low m6A scores had the worst prognosis (Fig. 4G). Nevertheless, we know that the effect of TMB on cancer patients is double-sided. In our results, high m6A score and high TMB both showed better prognosis, while the inverse association between TMB and m6A score seems puzzling, but it is not contradictory since the overall outcome is usually caused by multiple biological factors. A single factor of TMB is not sufficient to alter the final outcome in our patients.

Additionally, we assessed the gene mutation status of 406 cases in the m6A score groups via Maftools (Fig. 4H and I). From the results we noticed that the to-
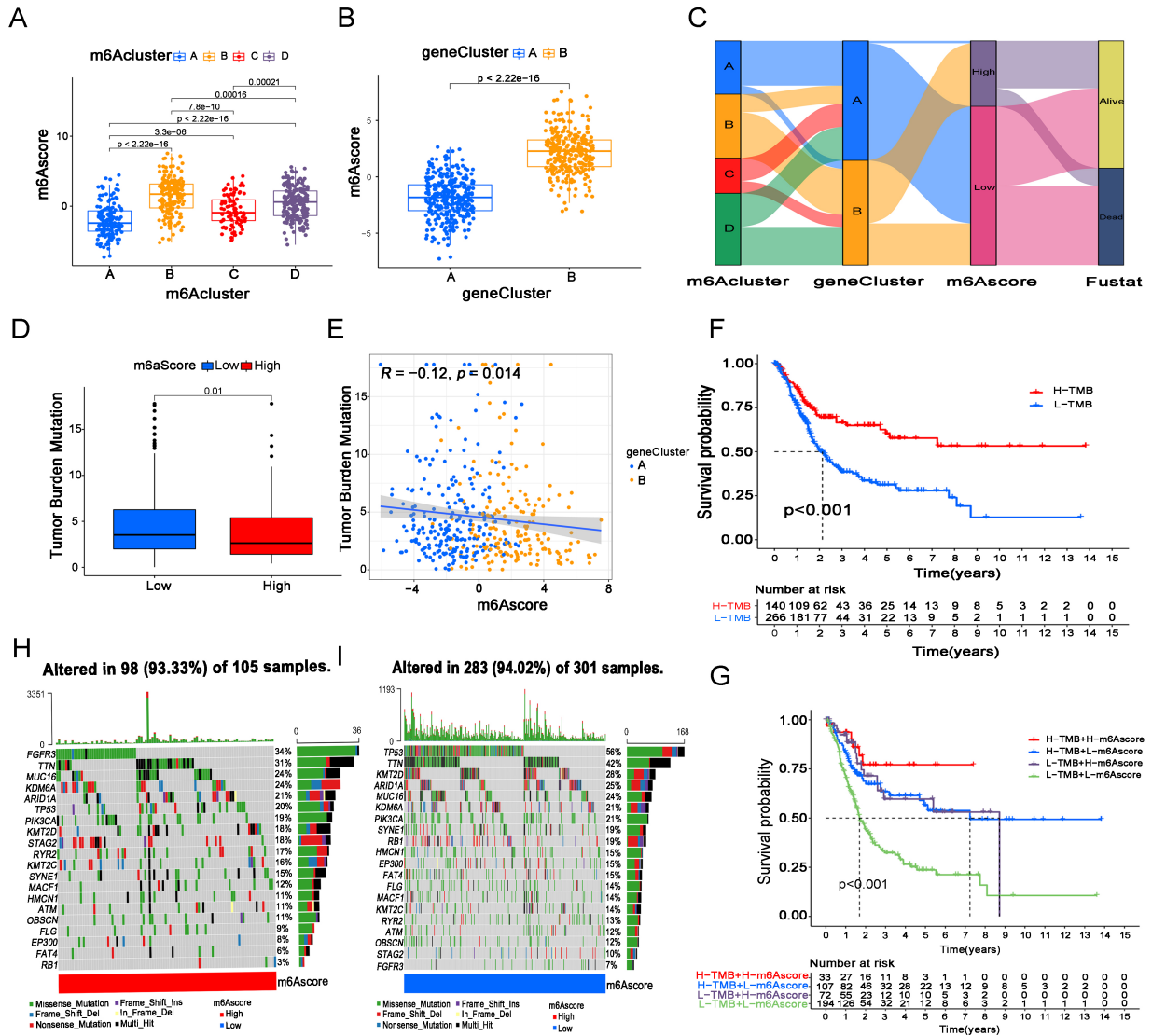
Fig. 4. The m6A score is closely related to TMB and gene mutations in BC patients. (A) m6A score levels in m6A cluster groups. (B) m6A score levels in gene clusters. (C) Corresponding relations between the m6A cluster, gene cluster, m6A score and Fustat in our patients. (D) TMB levels in the m6A score groups. (E) The correlations between TMB levels and m6A score. (F) Kaplan-Meier analysis of OS in patients with high and low TMB levels. (G) Kaplan-Meier analysis for OS in cases with four combinations that consisted of different TMB levels and different m6A scores. (H, I) The top 20 mutant genes in the HS (H) and LS groups (I).

tal mutant frequencies between HS group and LS group were similar (93.33% vs 94.02%), but FGFR3 was the most common mutant gene in cases from HS group, while TP53 in LS group. The differences in gene mutation status between m6A score groups could partly explain the different outcomes of cases in different groups.

3.5. The LS group predicts a higher risk of immune escape in BC patients

Furthermore, we assessed the correlation of the m6A

score with tumor immunity in BC. According to the results, we found that the m6A score was closely related to immune cell infiltration, and the LS group had higher infiltration of Treg cells and lower infiltration of CD8+ T cells than the HS group (Fig. 5A and B). Meanwhile, iDC, monocyte, Tcm and NK CD56bright cell infiltration was lower in the LS group than in the HS group and was positively correlated with the m6A score (Supplementary Fig. 6A–D). These findings suggested that patients in the LS group might have poorer immune function. Then, we examined the levels of the im-
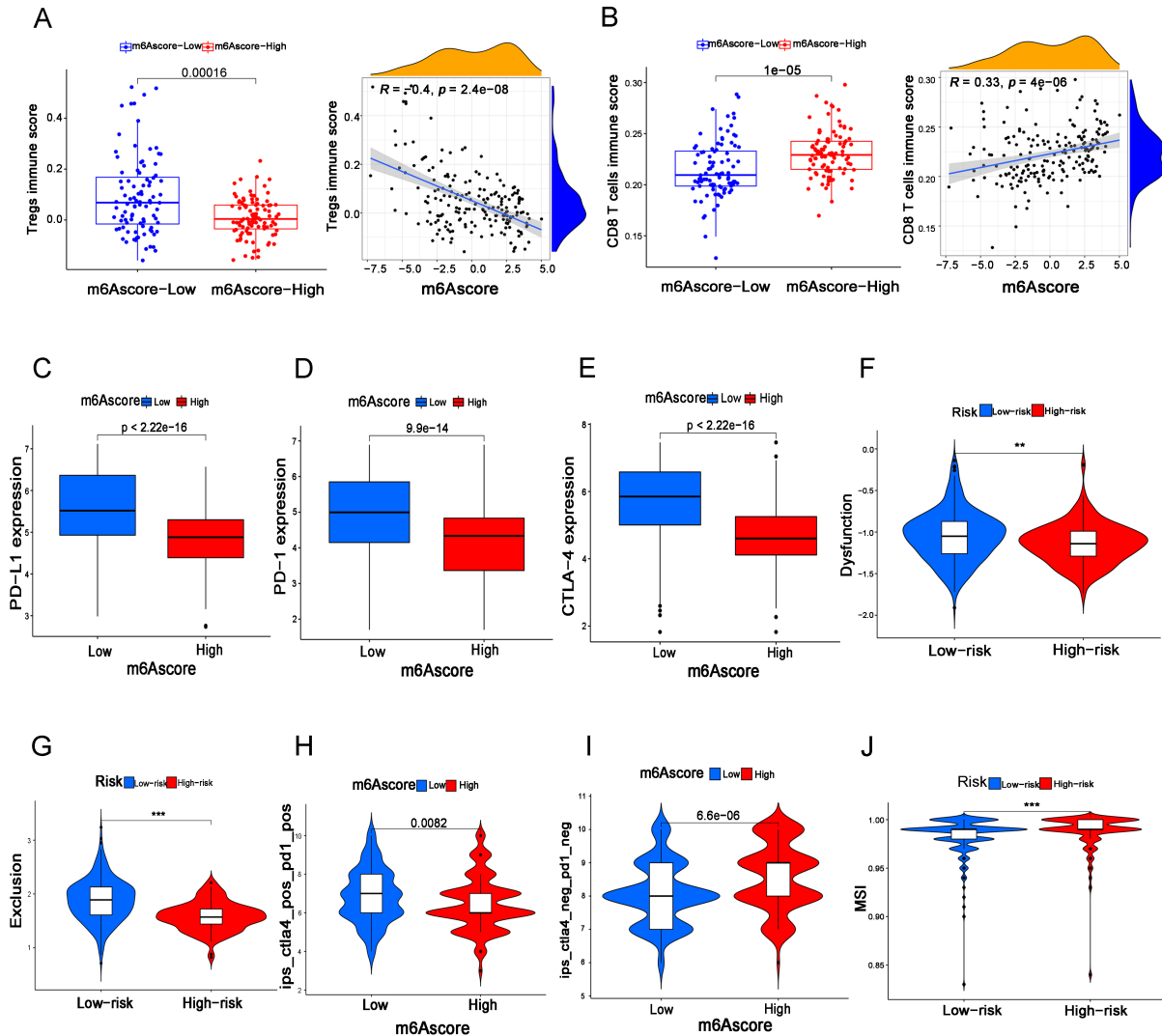
Fig. 5. The LS group predicts a higher risk of immune escape in BC patients. (A, B) The immune score of Treg cells (A) and CD8+ T (B) cells in the m6A score groups and correlations between immune score and m6A score. (C–E) The expression of PD-L1, PD-1 and CTLA4 between the HS and LS groups. (F–I) The immune dysfunction score (F), immune exclusion score (G), PD-1 and PD-L1 immunotherapy effect score (H), and negative PD-1 and PD-L1 immunotherapy effect score (I) between the HS and LS groups. (J) The MSI status between the HS and LS groups.

mune checkpoints PDL1, PD1 and CTLA4 in the m6A score groups. The results showed that these checkpoints were upregulated in the LS group compared to the HS group, which indicated that cases in the LS group had a higher risk of immune escape (Fig. 5C–E). In addition, a higher immune dysfunction score and immune exclusion score were identified in the LS group, which further demonstrated that the LS group was associated with a higher risk of immune escape in BC (Fig. 5F and G). Surprisingly, we found that when the patients were treated with PD-1 and PD-L1 immunotherapy, the LS group achieved a better therapeutic effect than the HS group. In contrast, when patients were treated with neg-

ative PD-1 and PD-L1 immunotherapy, the HS group achieved a better therapeutic effect than the LS group (Fig. 5H and I). In addition, we found that cases in the HS group had higher microsatellite instability (MSI), which might suggest a possible method for the gene detection of BC (Fig. 5J). These results suggested that the LS group had a higher risk of immune escape than the HS group and might gain more benefit from ICIs.

3.6. Experimental verification of m6A related gene and prognosis of bladder cancer

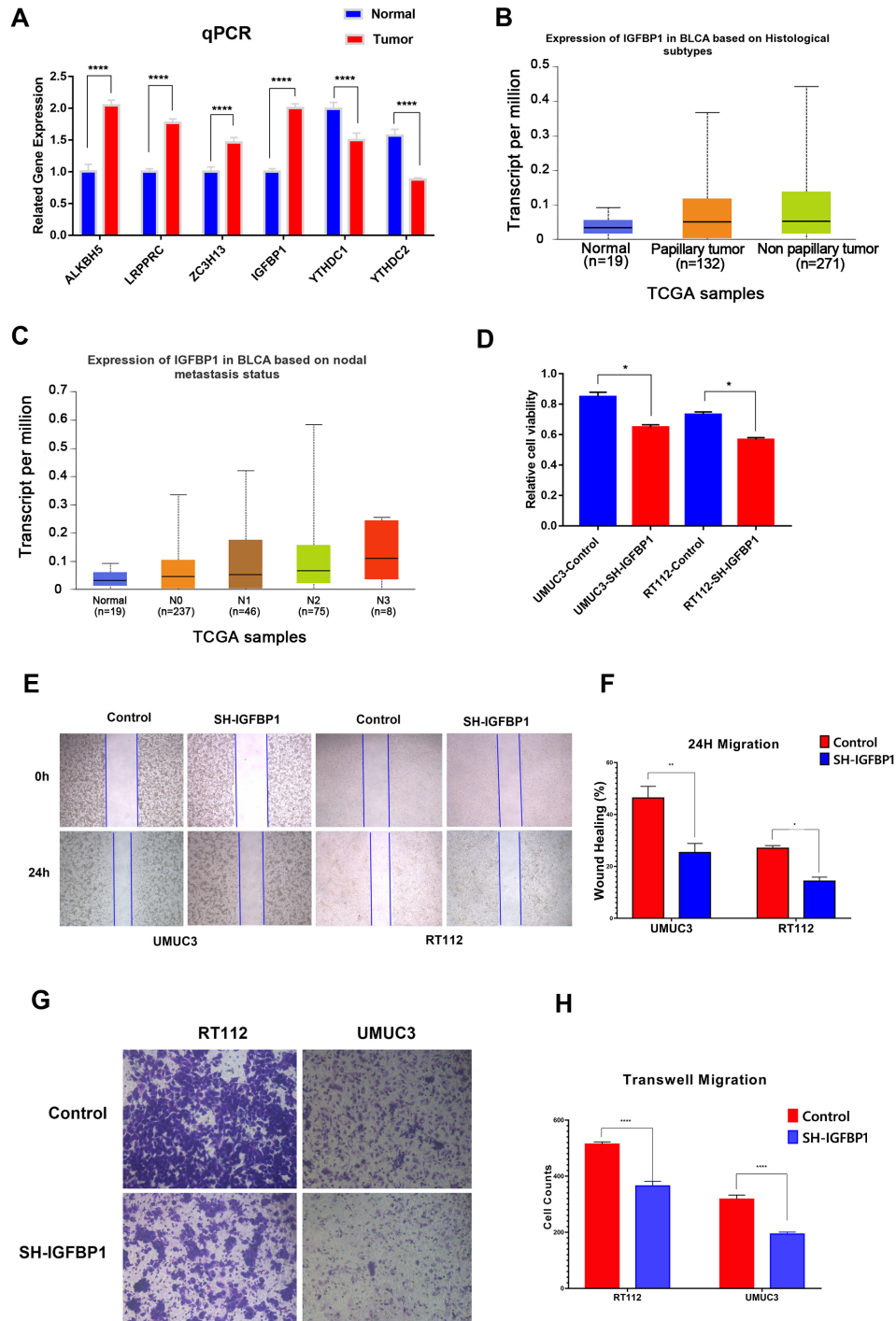In this work, we identified a total of six m6A re-

Fig. 6. Experimental verification of m6A related gene and prognosis of bladder cancer. A: The gene expression of ALKBH5, ZC3H13, LRPPRC, IGFBP1, YTHDC1 and YTHDC2 in bladder cancer tissues and adjacent normal tissues was measured by qPCR. B: CCK8 was used to determine the growth activity in the IGFBP1 knockdown group and empty vector group of bladder cancer cells. C and D: Gene expression levels of IGFBP1 in different groups. E and F: A wound healing assay was used to measure the migration ability of UMUC3 and RT112 cells in the IGFBP1 knockdown group and empty vector group. G and H Transwell assays were used to measure the migration ability of UMUC3 and RT112 cells in the IGFBP1 knockdown group and empty vector group.

lated genes that were both associated with overall survival and disease-specific survival, of which ALKBH5, ZC3H13, LRPPRC, IGFBP1 were associated with poor survival and YTHDC1 and YTHDC2 were associated with better survival. Furthermore, qPCR showed that the gene expression of ALKBH5, ZC3H13, LRPPRC, IGFBP1 in bladder cancer tissues was significantly higher than that in normal tissues, and YTHDC1 and YTHDC2 in bladder cancer tissues was significantly lower than that in normal tissues (Fig. 6A).

Among the six m6A related genes, of which ALKBH5, LRPPRC and YTHDC1 have been clearly reported to be associated with bladder cancer in the literature, but the biological roles of ZC3H13, IGFBP1 and YTHDC2 in bladder cancer are poorly understood [18,19,20,21,22,23,24,25,26]. Furthermore, we analyzed ZC3H13, IGFBP1 and YTHDC2 in TCGA dataset, and found that IGFBP1 had a higher expression level in non primary bladder cancer and high lymph node metastasis patients (Fig. 6B and C), while ZC3H13 and YTHDC2 did not observe this trend. These findings suggest that IGFBP1 may be more related to the poor prognosis of bladder cancer. Therefore, we selected IGFBP1 for further experimental verification. The results showed that the growth activity of bladder cancer cells in the IGFBP1 knockdown group was significantly inhibited in UMUC3 and RT112 cells compared to that in the empty vector transfection group (Fig. 6E and F). In addition, in UMUC3 and RT112 cells, the metastatic ability of the IGFBP1 knockdown group was significantly inhibited compared with that of the empty vector transfection group (Fig. 6G and H). These results suggested the important role of m6A-related genes, especially IGFBP1, in the prognosis of bladder cancer.

4. Discussion

At present, increasing evidence suggests the important roles of m6A in the development of tumors. It has been reported that VIRMA is the most commonly up-regulated m6A gene in BC and is essential to the m6A of mRNA in the 3' untranslated regions (3'UTRs) and around the stop codon, as well as alternative polyadenylation [27]. Meanwhile, the expression of YTHDF2 was suggested to correlate with a good prognosis in BC [28]. These results implied the important roles of m6A genes in BC. Rencently, Liu et al. determined three different N6-methyladenosine modification patterns and explored the inherent relationships between

these modification patterns and multiomic tumor characteristics [17], which revealed the important roles of m6A methylation modification patterns in bladder cancer. However, due to the complex functions of m6A related genes, more evidence needs to be further explored in bladder cancer. In this work, we has drawn many new and valuable findings that differ from Liu et al.'s study. First, we have proposed a new m6A clustering scheme and performed corresponding functional enrichment analysis, immune infiltration analysis for BC patients. In addition, we have determined a new genotyping results based on m6A related genes and performed corresponding survival prognosis analysis for BC patients. Moreover, based on the m6A score, we performed disease-specific survival analysis, tumor mutational burden analysis, gene mutation characteristics analysis, immune exclusion analysis, immune dysfunction analysis, microsatellite instability (MSI) analysis, CD8+ T cell and Trges analysis, etc. for BC patients. These results are crucial to further reveal the biological function of m6A related genes in bladder cancer. What's more, we selected m6A related genes (ALKBH5, ZC3H13, LRPPRC, IGFBP1, YTHDC1 and YTHDC2) for experimental verification, which further strengthened the evidence of m6A related genes and the prognosis of bladder cancer.

According to our results, METTL3 was the most frequently mutated m6A gene in BC, and different mutation statuses of METTL3 could influence the expression levels of other m6A genes, which may partly contribute to the prognosis of BC. METTL3 has been reported to anticipate tumorigenesis by playing roles as a m6A "writer", either as an oncogene or a suppressor gene, in many types of cancers [29]. In addition, it is suggested that the expression level of METTL3 was upregulated in BC and improved mRNA translation levels through YTHDF1/3 binding, which was regulated by METTL3 m6A modification targeted to CDCP1 and ITGA6 [30, 31]. In addition, METTL3 was found to function as an oncogene that could promote tumor proliferation in BC via the accumulation of pri-miR221/222 mutations in the m6A process [32]. Moreover, a study indicated that METTL3 might improve BC progression and angiogenesis via tyrosine kinase endothelial and vascular endothelial growth factor A, which could be a potential therapeutic target [33]. In summary, METTL3 is a vital m6A gene and plays important roles in tumorigenesis in BC. According to the m6A cluster, we comprehensively analyzed m6A gene functions and pathways in BC. We noticed that DNA replication function and IGF-related proteins and pathways were strongly associated with

the m6A process. The IGF system is believed to play important roles in cell proliferation, differentiation and metabolism [34]. Commonly, the level of the IGF system is higher in malignant cells and tissues, which is associated with a poor prognosis [32]. IGFBPs are ligands of IGF proteins that help IGF combine with IGF receptors. A few studies revealed that low levels of IGFBPs were found in BC because of methylation in IGFBP genes, while the mechanisms of m6A suppression of the IGF system in BC remain rarely explored [35,36]. Accordingly, we believe that it is worth further investigating the relationship between the m6A process and IGF systems in cancers.

Furthermore, according to our m6A clusters, a total of 11 OSRGs (CRTAC1, SMAD6, CDC25B, ZNF552, KLHL3, TPX2, WDR62, MTHFD2, PAQR4, KPNA2 and CLIC4) were identified in our patients. Among these 11 genes, CRTAC1, SMAD6, KLHL3 and ZNF552 were downregulated in gene cluster A, which had a poorer prognosis. A study reported that CRTAC1 inhibits the malignant behaviors of BC cells by mediating the downstream gene Yin Yang 1 (YY1) to inactivate TGF-β [37]. Downregulation of SMAD6 expression could inhibit the tumor cell cycle in colorectal cancer [38]. Interestingly, KLHL3 does not seem to be involved in tumorigenesis but was found to participate in hypertension by inducing WNK4 ubiquitination [39]. In addition, there are no reports about ZNF552 as a tumor-related gene, although it functions as a zinc finger protein that can regulate the transcription levels of other proteins [40]. Meanwhile, the other 7 genes were upregulated in gene cluster A. It has been reported that TPX2 promotes angiogenesis via secretory autophagy in BC [41]. Then, a high level of WDR62 was found to be associated with tumor aggressiveness, while knockdown of WDR62 could induce BC cell apoptosis [42]. In addition, MTHFD2 was revealed to mediate the cell cycle so that it could initiate CDK2 to induce the progression of BC [43]. Moreover, a study suggested that depletion of PAQR4 could improve the efficacy of chemotherapy in non-small cell lung cancer [44]. Nevertheless, there was evidence that a high level of KPNA2 correlated with a high risk of progression in the early stage of BC [45]. Similarly, a high level of CLIC4 was found to improve epithelial-mesenchymal transition in gastric cancer [46]. Moreover, CDC25B protein was found to be downregulated when treated with a traditional Chinese medicine, which correlated with good drug efficacy in inhibiting BC [47]. Overall, the joint effect of these 11 genes has caused different prognoses between gene clusters A and B; somehow,

the biological effects of these 11 genes in BC are still unclear and remain to be further explored in the future.

In our study, we found that patients with high TMB levels had a better prognosis, and the LS group not only had a poor prognosis but also had a high TMB level. The TMB level is considered a biomarker to predict the immunotherapy response in many types of cancers, including BC, and a high TMB level is believed to be associated with a better immunotherapeutic response [48]. A better immunotherapy effect in the high TMB group may be the reason for the better prognosis. We could not fully understand the mechanism by which the LS group had high TMB levels, but we know that organisms are so complex and that TMB levels could not influence the final outcome as a single factor in our patients.

Importantly, we discovered the potential value of the m6A score in immune escape and prediction of the effect of immunotherapy. First, we found that TP53 was the most frequently mutated gene in the LS group. The normal function of TP53 is mainly as a suppressor gene, which could initiate cell apoptosis when cell cycle arrest or DNA damage occurs [49]. Meanwhile, TP53 is reported as the most common mutant gene in human malignancy, with possibilities to predict prognosis and immunotherapeutic response in BC [16,50]. Accordingly, we speculated that the high TP53 mutation rate in the LS group could be the key reason for the poor prognosis. Moreover, we further found that the m6A score was negatively correlated with regulatory T cells (Tregs) and positively correlated with CD8+ T cells. Tregs are commonly believed to play roles not only in the suppression of autoimmune disease but also in tumorigenesis. A report suggested that high Treg infiltration correlated with poor OS in many solid cancers [51]. Another study indicated that depletion of Tregs could help improve survival in canine BC via blockade of CCR4 [52]. Moreover, CD8+ T cells are the most common immune killer cells in cancer, and CD8+ T cells were suggested to be a potential biomarker for several therapeutic methods in BC, including immune checkpoint therapy, monoclonal antibodies, and vaccines [53]. These results demonstrated the important value of the m6A score in evaluating immune function and may help us further understand the mechanisms for the better prognosis of patients in the HS group. Surprisingly, the LS group showed higher expression of checkpoints such as PDL1, PD1 and CTLA4 than the HS group. According to a previous study, high expression levels of these checkpoints might lead to effective T-cell inactivation and immune escape, yet patients with high levels of checkpoints could gain more

benefit from immunotherapy [54,55]. Accordingly, we speculated that patients from the LS group could be more sensitive to immunotherapy in BC, and these differentially expressed checkpoint levels could lead to more possibilities for immune escape.

5. Conclusions

In conclusion, we demonstrated the important roles of m6A MRGs in predicting prognosis, TMB status, TP53 mutation, immune functions and immunotherapeutic response in BC. These findings may also provide new potential targets for the precision treatment of BC.

Conflict of interest

The authors have no relevant financial or nonfinancial interests to disclose.

Author contributions

Conception: Minghua Ren, Wanhai Xu; Interpretation or analysis of data: Yang Liu, Zhongqi Pang, Jianshe Wang; Preparation of the manuscript: Jinfeng Wang, Bo Ji; Revision for important intellectual content: Yidan Xu, Jiaxin He; Supervision: Lu Zhang, Yansong Han, Lingkun Shen.

Data availability statement

All data in this study are available in the TCGA data portal (https://tcga-data.nci.nih.gov/tcga/) and GEO data portal (http://www.ncbi.nlm.nih.gov/geo/).

Ethics approval

Not applicable.

Supplementary data

The supplementary files are available to download from http://dx.doi.org/10.3233/CBM-230286.

References

[1] F. Bray, J. Ferlay, I. Soerjomataram, R.L. Siegel, L.A. Torre and A. Jemal, Global cancer statistics 2018: GLOBOCAN estimates of incidence and mortality worldwide for 36 cancers in 185 countries, *CA Cancer J Clin* **68** (2018), 394–424. doi: 10.3322/caac.21492.

[2] A. Richters, K.K.H. Aben and L.A.L.M. Kiemeney, The global burden of urinary bladder cancer: An update, *World J Urol* **38** (2020), 1895–1904. doi: 10.1007/s00345-019-02984-4.

[3] A.T. Lenis, P.M. Lec, K. Chamie and M.D. Mshs, Bladder cancer: A review, *JAMA* **324** (2020), 1980–1991. doi: 10.1001/jama.2020.17598.

[4] S.J. Crabb and J. Douglas, The latest treatment options for bladder cancer, *Br Med Bull* **128** (2018), 85–95. doi: 10.1093/bmb/ldy034.

[5] Y. Yue, J. Liu and C. He, RNA N6-methyladenosine methylation in post-transcriptional gene expression regulation, *Genes Dev* **29** (2015), 1343–1355. doi: 10.1101/gad.262766.115.

[6] T. Sun, R. Wu and L. Ming, The role of m6A RNA methylation in cancer, *Biomed Pharmacother* **112** (2019), 108613. doi: 10.1016/j.biopha.2019.108613.

[7] A. Du, S. Li, Y. Zhou, C. Disoma, Y. Liao, Y. Zhang, Z. Chen, Q. Yang, P. Liu, S. Liu, Z. Dong, A. Razzaq, S. Tao, X. Chen, Y. Liu, L. Xu, Q. Zhang, S. Li, J. Peng and Z. Xia, M6A-mediated upregulation of circMDK promotes tumorigenesis and acts as a nanotherapeutic target in hepatocellular carcinoma, *Mol Cancer* **21** (2022), 109. doi: 10.1186/s12943-022-01575-z.

[8] H. Han, G. Fan, S. Song, Y. Jiang, C. Qian, W. Zhang, Q. Su, X. Xue, W. Zhuang and B. Li, piRNA-30473 contributes to tumorigenesis and poor prognosis by regulating m6A RNA methylation in DLBCL, *Blood* **137** (2021), 1603–1614. doi: 10.1182/blood.2019003764.

[9] Q. Lan, P.Y. Liu, J.L. Bell, J.Y. Wang, S. Hüttelmaier, X.D. Zhang, L. Zhang and T. Liu, The Emerging Roles of RNA m6A Methylation and Demethylation as Critical Regulators of Tumorigenesis, Drug Sensitivity, and Resistance, *Cancer Res* **81** (2021), 3431–3440. doi: 10.1158/0008-5472.CAN-20-4107.

[10] M. Cheng, L. Sheng, Q. Gao, Q. Xiong, H. Zhang, M. Wu, Y. Liang, F. Zhu, Y. Zhang, X. Zhang, Q. Yuan and Y. Li, The m6A methyltransferase METTL3 promotes bladder cancer progression via AFF4/NF-κB/MYC signaling network, *Oncogene* **38** (2019), 3667–3680. doi: 10.1038/s41388-019-0683-z.

[11] J. Li, H. Xie, Y. Ying, H. Chen, H. Yan, L. He, M. Xu, X. Xu,

Z. Liang, B. Liu, X. Wang, X. Zheng and L. Xie, YTHDF2 mediates the mRNA degradation of the tumor suppressors to induce AKT phosphorylation in N6-methyladenosine-dependent way in prostate cancer, *Mol Cancer* **19** (2020), 152. doi: 10.1186/s12943-020-01267-6.

[12] L. Tao, X. Mu, H. Chen, D. Jin, R. Zhang, Y. Zhao, J. Fan, M. Cao and Z. Zhou, FTO modifies the m6A level of MALAT and promotes bladder cancer progression, *Clin Transl Med* **11** (2021), e310. doi: 10.1002/ctm2.310.

[13] D. Song, T. Powles, L. Shi, L. Zhang, M.A. Ingersoll and Y.-J. Lu, Bladder cancer, a unique model to understand cancer immunity and develop immunotherapy approaches, *J Pathol* **249** (2019), 151–165. doi: 10.1002/path.5306.

[14] A. Lopez-Beltran, A. Cimadamore, A. Blanca, F. Massari, N. Vau, M. Scarpelli, L. Cheng and R. Montironi, Immune checkpoint inhibitors for the treatment of bladder cancer, *Cancers (Basel)* **13** (2021), 131. doi: 10.3390/cancers13010131.

[15] R.M. Samstein, C.-H. Lee, A.N. Shoushtari, M.D. Hellmann, R. Shen, Y.Y. Janjigian, D.A. Barron, A. Zehir, E.J. Jordan, A. Omuro, T.J. Kaley, S.M. Kendall, R.J. Motzer, A.A. Hakimi, M.H. Voss, P. Russo, J. Rosenberg, G. Iyer, B.H. Bochner, D.F. Bajorin, H.A. Al-Ahmadie, J.E. Chaft, C.M. Rudin, G.J. Riely, S. Baxi, A.L. Ho, R.J. Wong, D.G. Pfister, J.D. Wolchok, C.A. Barker, P.H. Gutin, C.W. Brennan, V. Tabar, I.K. Mellinghoff, L.M. DeAngelis, C.E. Ariyan, N. Lee, W.D. Tap, M.M. Gounder, S.P. D'Angelo, L. Saltz, Z.K. Stadler, H.I. Scher, J. Baselga, P. Razavi, C.A. Klebanoff, R. Yaeger, N.H. Segal, G.Y. Ku, R.P. DeMatteo, M. Ladanyi, N.A. Rizvi, M.F. Berger, N. Riaz, D.B. Solit, T.A. Chan and L.G.T. Morris, Tumor mutational load predicts survival after immunotherapy across multiple cancer types, *Nat Genet* **51** (2019), 202–206. doi: 10.1038/s41588-018-0312-8.

[16] X. Wu, D. Lv, C. Cai, Z. Zhao, M. Wang, W. Chen and Y. Liu, A TP53-associated immune prognostic signature for the prediction of overall survival and therapeutic responses in muscle-invasive bladder cancer, *Front Immunol* **11** (2020), 590618. doi: 10.3389/fimmu.2020.590618.

[17] J. Liu, J. Wang, M. Wu, W. Zhang, L. Meng, J. Wang, Z. Lv, H. Xia, Y. Zhang and J. Wang, Comprehensive analysis of N6-methyladenosine modification patterns associated with multi-omic characteristics of bladder cancer, *Front Med (Lausanne)* **8** (2021), 757432. doi: 10.3389/fmed.2021.757432.

[18] W.-S. Wei, N. Wang, M.-H. Deng, P. Dong, J.-Y. Liu, Z. Xiang, X.-D. Li, Z.-Y. Li, Z.-H. Liu, Y.-L. Peng, Z. Li, L.-J. Jiang, K. Yao, Y.-L. Ye, W.-H. Lu, Z.-L. Zhang, F.-J. Zhou, Z.-W. Liu, D. Xie and C.-P. Yu, LRPPRC regulates redox homeostasis via the circANKHD1/FOXM1 axis to enhance bladder urothelial carcinoma tumorigenesis, *Redox Biol* **48** (2021), 102201. doi: 10.1016/j.redox.2021.102201.

[19] L. Huang, G. Chen, J. He and P. Wang, ZC3H13 reduced DUOX1-mediated ferroptosis in laryngeal squamous cell carcinoma cells through m6A-dependent modification, *Tissue Cell* **84** (2023), 102187. doi: 10.1016/j.tice.2023.102187.

[20] Y.-W. Lin, X.-F. Weng, B.-L. Huang, H.-P. Guo, Y.-W. Xu and Y.-H. Peng, IGFBP-1 in cancer: Expression, molecular mechanisms, and potential clinical implications, *Am J Transl Res* **13** (2021), 813–832.

[21] B. Yan, X. Li, M. Peng, Y. Zuo, Y. Wang, P. Liu, W. Ren and X. Jin, The YTHDC1/GLUT3/RNF183 axis forms a positive feedback loop that modulates glucose metabolism and bladder cancer progression, *Exp Mol Med* **55** (2023), 1145–1158. doi: 10.1038/s12276-023-00997-z.

[22] Y. Su, B. Wang, J. Huang, M. Huang and T. Lin, YTHDC1 positively regulates PTEN expression and plays a critical role

in cisplatin resistance of bladder cancer, *Cell Prolif* **56** (2023), e13404. doi: 10.1111/cpr.13404.

[23] L. Ma, T. Chen, X. Zhang, Y. Miao, X. Tian, K. Yu, X. Xu, Y. Niu, S. Guo, C. Zhang, S. Qiu, Y. Qiao, W. Fang, L. Du, Y. Yu and J. Wang, The m6A reader YTHDC2 inhibits lung adenocarcinoma tumorigenesis by suppressing SLC7A11-dependent antioxidant function, *Redox Biol* **38** (2021), 101801. doi: 10.1016/j.redox.2020.101801.

[24] J. Zhang, S. Guo, H.-Y. Piao, Y. Wang, Y. Wu, X.-Y. Meng, D. Yang, Z.-C. Zheng and Y. Zhao, ALKBH5 promotes invasion and metastasis of gastric cancer by decreasing methylation of the lncRNA NEAT1, *J Physiol Biochem* **75** (2019), 379–389. doi: 10.1007/s13105-019-00690-8.

[25] H. Yu, X. Yang, J. Tang, S. Si, Z. Zhou, J. Lu, J. Han, B. Yuan, Q. Wu, Q. Lu and H. Yang, ALKBH5 Inhibited Cell Proliferation and Sensitized Bladder Cancer Cells to Cisplatin by m6A-CK2α-Mediated Glycolysis, *Mol Ther Nucleic Acids* **23** (2021), 27–41. doi: 10.1016/j.omtn.2020.10.031.

[26] S. Jin, M. Li, H. Chang, R. Wang, Z. Zhang, J. Zhang, Y. He and H. Ma, The m6A demethylase ALKBH5 promotes tumor progression by inhibiting RIG-I expression and interferon alpha production through the IKKε/TBK1/IRF3 pathway in head and neck squamous cell carcinoma, *Mol Cancer* **21** (2022), 97. doi: 10.1186/s12943-022-01572-2.

[27] Y. Yue, J. Liu, X. Cui, J. Cao, G. Luo, Z. Zhang, T. Cheng, M. Gao, X. Shu, H. Ma, F. Wang, X. Wang, B. Shen, Y. Wang, X. Feng, C. He and J. Liu, VIRMA mediates preferential m6A mRNA methylation in 3'UTR and near stop codon and associates with alternative polyadenylation, *Cell Discov* **4** (2018), 10. doi: 10.1038/s41421-018-0019-0.

[28] B. Zheng, J. Wang, G. Zhao, X. Chen, Z. Yao, Z. Niu and W. He, A new m6A methylation-related gene signature for prognostic value in patient with urothelial carcinoma of the bladder, *Biosci Rep* **41** (2021), BSR20204456. doi: 10.1042/BSR20204456.

[29] C. Zeng, W. Huang, Y. Li and H. Weng, Roles of METTL3 in cancer: Mechanisms and therapeutic targeting, *J Hematol Oncol* **13** (2020), 117. doi: 10.1186/s13045-020-00951-w.

[30] H. Jin, X. Ying, B. Que, X. Wang, Y. Chao, H. Zhang, Z. Yuan, D. Qi, S. Lin, W. Min, M. Yang and W. Ji, N6-methyladenosine modification of ITGA6 mRNA promotes the development and progression of bladder cancer, *EBioMedicine* **47** (2019), 195–207. doi: 10.1016/j.ebiom.2019.07.068.

[31] F. Yang, H. Jin, B. Que, Y. Chao, H. Zhang, X. Ying, Z. Zhou, Z. Yuan, J. Su, B. Wu, W. Zhang, D. Qi, D. Chen, W. Min, S. Lin and W. Ji, Dynamic m6A mRNA methylation reveals the role of METTL3-m6A-CDCP1 signaling axis in chemical carcinogenesis, *Oncogene* **38** (2019), 4755–4772. doi: 10.1038/s41388-019-0755-0.

[32] J. Han, J.-Z. Wang, X. Yang, H. Yu, R. Zhou, H.-C. Lu, W.-B. Yuan, J.-C. Lu, Z.-J. Zhou, Q. Lu, J.-F. Wei and H. Yang, METTL3 promote tumor proliferation of bladder cancer by accelerating pri-miR221/222 maturation in m6A-dependent manner, *Mol Cancer* **18** (2019), 110. doi: 10.1186/s12943-019-1036-9.

[33] G. Wang, Y. Dai, K. Li, M. Cheng, G. Xiong, X. Wang, S. Chen, Z. Chen, J. Chen, X. Xu, R.-S. Ling, L. Peng and D. Chen, Deficiency of Mettl3 in Bladder Cancer Stem Cells Inhibits Bladder Cancer Progression and Angiogenesis, *Front Cell Dev Biol* **9** (2021), 627706. doi: 10.3389/fcell.2021.627706.

[34] F. Hakuno and S.-I. Takahashi, IGF1 receptor signaling pathways, *J Mol Endocrinol* **61** (2018), T69–T86. doi: 10.1530/JME-17-0311.

[35] S.F. Shariat, J. Kim, C. Nguyen, T.M. Wheeler, S.P. Lerner and K.M. Slawin, Correlation of preoperative levels of IGF-I and IGFBP-3 with pathologic parameters and clinical outcome in patients with bladder cancer, *Urology* **61** (2003), 359–364. doi: 10.1016/s0090-4295(02)02253-7.

[36] F. Christoph, S. Weikert, C. Kempkensteffen, H. Krause, M. Schostak, K. Miller and M. Schrader, Regularly methylated novel pro-apoptotic genes associated with recurrence in transitional cell carcinoma of the bladder, *Int J Cancer* **119** (2006), 1396–1402. doi: 10.1002/ijc.21971.

[37] J. Yang, L. Fan, X. Liao, G. Cui and H. Hu, CRTAC1 (Cartilage acidic protein 1) inhibits cell proliferation, migration, invasion and epithelial-mesenchymal transition (EMT) process in bladder cancer by downregulating Yin Yang 1 (YY1) to inactivate the TGF-β pathway, *Bioengineered* **12** (2021), 9377–9389. doi: 10.1080/21655979.2021.1974645.

[38] Z. Bayat, Z. Ghaemi, M. Behmanesh and B.M. Soltani, Hsa-miR-186-5p regulates TGFβ signaling pathway through expression suppression of SMAD6 and SMAD7 genes in colorectal cancer, *Biol Chem* **402** (2021), 469–480. doi: 10.1515/hsz-2019-0407.

[39] M. Wakabayashi, T. Mori, K. Isobe, E. Sohara, K. Susa, Y. Araki, M. Chiga, E. Kikuchi, N. Nomura, Y. Mori, H. Matsuo, T. Murata, S. Nomura, T. Asano, H. Kawaguchi, S. Nonoyama, T. Rai, S. Sasaki and S. Uchida, Impaired KLHL3-mediated ubiquitination of WNK4 causes human hypertension, *Cell Rep* **3** (2013), 858–868. doi: 10.1016/j.celrep.2013.02.024.

[40] Y. Deng, B. Liu, X. Fan, Y. Wang, M. Tang, X. Mo, Y. Li, Z. Ying, Y. Wan, N. Luo, J. Zhou, X. Wu and W. Yuan, ZNF552, a novel human KRAB/C2H2 zinc finger protein, inhibits AP-1- and SRE-mediated transcriptional activity, *BMB Rep* **43** (2010), 193–198. doi: 10.5483/bmbrep.2010.43.3.193.

[41] X. Li, Z. Wei, H. Yu, Y. Xu, W. He, X. Zhou and X. Gou, Secretory autophagy-induced bladder tumour-derived extracellular vesicle secretion promotes angiogenesis by activating the TPX2-mediated phosphorylation of the AURKA-PI3K-AKT axis, *Cancer Lett* **523** (2021), 10–28. doi: 10.1016/j.canlet.2021.09.036.

[42] S. Sugita, H. Yoshino, M. Yonemori, K. Miyamoto, R. Matsushita, T. Sakaguchi, T. Itesako, S. Tatarano, M. Nakagawa and H. Enokida, Tumor-suppressive microRNA-223 targets WDR62 directly in bladder cancer, *Int J Oncol* **54** (2019), 2222–2236. doi: 10.3892/ijo.2019.4762.

[43] X. Liu, S. Liu, C. Piao, Z. Zhang, X. Zhang, Y. Jiang and C. Kong, Non-metabolic function of MTHFD2 activates CDK2 in bladder cancer, *Cancer Sci* **112** (2021), 4909–4919. doi: 10.1111/cas.15159.

[44] P. Xu, L. Jiang, Y. Yang, M. Wu, B. Liu, Y. Shi, Q. Shen, X. Jiang, Y. He, D. Cheng, Q. Xiong, Z. Yang, L. Duan, J. Lin, S. Zhao, P. Shi, C. Yang and Y. Chen, PAQR4 promotes chemoresistance in non-small cell lung cancer through inhibiting Nrf2 protein degradation, *Theranostics* **10** (2020), 3767–3778. doi: 10.7150/thno.43142.

[45] J.B. Jensen, P.P. Munksgaard, C.M. Sørensen, N. Fristrup, K. Birkenkamp-Demtroder, B.P. Ulhøi, K.M.-E. Jensen, T.F. Ørntoft and L. Dyrskjøt, High expression of karyopherin-α2 defines poor prognosis in non-muscle-invasive bladder cancer and in patients with invasive bladder cancer undergoing radical cystectomy, *Eur Urol* **59** (2011), 841–848. doi: 10.1016/j.eururo.2011.01.048.

[46] B. Wang, J. Zheng, Q. Chen, C. Wu, Y. Li, X.-Y. Yu, B. Liu, C. Liang, S.-B. Liu, H. Ding, S. Wang, T. Xue, D. Song, Z. Lei, H.M. Amin, Y.-H. Song and J. Zhou, CLIC4 abrogation promotes epithelial-mesenchymal transition in gastric cancer, *Carcinogenesis* **41** (2020), 841–849. doi: 10.1093/carcin/bgz156.

[47] T.-T. Ou, C.-H. Wu, J.-D. Hsu, C.-C. Chyau, H.-J. Lee and C.-J. Wang, Paeonia lactiflora Pall inhibits bladder cancer growth involving phosphorylation of Chk2 *in vitro* and *in vivo*, *J Ethnopharmacol* **135** (2011), 162–172. doi: 10.1016/j.jep.2011.03.011.

[48] T.A. Chan, E. Yarchoan, E. Jaffee, C. Swanton, S.A. Quezada, A. Stenzinger and S. Peters, Development of tumor mutation burden as an immunotherapy biomarker: Utility for the oncology clinic, *Ann Oncol* **30** (2019), 44–56. doi: 10.1093/annonc/mdy495.

[49] P.B.S. Lai, T.-Y. Chi and G.G. Chen, Different levels of p53 induced either apoptosis or cell cycle arrest in a doxycycline-regulated hepatocellular carcinoma cell line *in vitro*, *Apoptosis* **12** (2007), 387–393. doi: 10.1007/s10495-006-0571-1.

[50] M.C. Ingaramo, J.A. Sánchez and A. Dekanty, Regulation and function of p53: A perspective from Drosophila studies, *Mech Dev* **154** (2018), 82–90. doi: 10.1016/j.mod.2018.05.007.

[51] H.M. Knochelmann, C.J. Dwyer, S.R. Bailey, S.M. Amaya, D.M. Elston, J.M. Mazza-McCrann and C.M. Paulos, When worlds collide: Th17 and Treg cells in cancer and autoimmunity, *Cell Mol Immunol* **15** (2018), 458–469. doi: 10.1038/s41423-018-0004-4.

[52] S. Maeda, K. Murakami, A. Inoue, T. Yonezawa and N. Matsuki, CCR4 Blockade Depletes Regulatory T Cells and Prolongs Survival in a Canine Model of Bladder Cancer, *Cancer Immunol Res* **7** (2019), 1175–1187. doi: 10.1158/2326-6066.CIR-18-0751.

[53] W. Zhu, Z. Zhao, B. Feng, W. Yu, J. Li, H. Guo and R. Yang, CD8+CD39+ T Cells Mediate Anti-Tumor Cytotoxicity in Bladder Cancer, *Onco Targets Ther* **14** (2021), 2149–2161. doi: 10.2147/OTT.S297272.

[54] T. Powles, P.H. O'Donnell, C. Massard, H.-T. Arkenau, T.W. Friedlander, C.J. Hoimes, J.L. Lee, M. Ong, S.S. Sridhar, N.J. Vogelzang, M.N. Fishman, J. Zhang, S. Srinivas, J. Parikh, J. Antal, X. Jin, A.K. Gupta, Y. Ben and N.M. Hahn, Efficacy and safety of durvalumab in locally advanced or metastatic urothelial carcinoma: Updated results from a phase 1/2 open-label study, *JAMA Oncol* **3** (2017), e172411. doi: 10.1001/jamaoncol.2017.2411.

[55] M.F. Krummel and J.P. Allison, CD28 and CTLA-4 have opposing effects on the response of T cells to stimulation, *J Exp Med* **182** (1995), 459–465. doi: 10.1084/jem.182.2.459.